Int. J. Solids Structures Vol. 29, No. 23, pp. 2855–2866, 1992
Printed in Great Britain.

0020-7683/92 $5.00 + .00

ELECTROMAGNETIC TWISTING OF A MINDLIN PLATE WITH A THROUGH CRACK

YASUHIDE SHINDO and YASUSHI ATOBE
Department of Materials Processing, Faculty of Engineering, Tohoku University, Aramaki-Aza-Aoba, Aoba-ku, Sendai 980, Japan

(*Received 5 December 1991; in revised form 11 May 1992*)

Abstract—This paper deals with the electromagneto-elastic problem of a fixed ended conducting plate of finite width with a through crack under a uniform electric current flow and a constant magnetic field. The study is based on Mindlin's theory of plate bending. The current flow is disturbed by the presence of the crack and the twisting moment is caused by the interaction between the magnetic field and the disturbed current. Fourier transforms are used to reduce the electromagneto-elastic problem to one involving the numerical solution of a system of simultaneous Fredholm integral equations. The problem concerning the electric current density field is also solved and reduced to a Fredholm integral equation of the second kind. The singular character and the detailed structure of the electric current densities and the stresses near the ends of the crack are determined in closed forms. Numerical results are given for the twisting moment intensity factor and the shear force intensity factor for several values of the geometrical parameters.

INTRODUCTION

Cracks in conducting materials under electromagnetic loading are a major problem in the structural design of the superconducting devices. By design, the components of the superconducting structures are most often used in environments with large electric currents and strong magnetic fields. Therefore, a better understanding of cracks under electromagnetic loading conditions is needed to guide the structural design and integrity assessment of the superconducting structures. The stress intensity factor approach of linear elastic fracture mechanics has proved to be very successful in predicting the unstable fracture of brittle solids (Murakami, 1986). When cracked conducting materials are subjected to electric current flows and magnetic fields, the same approach is expected to apply. Considerable work has been done to determine the stress field around a finite crack in an elastic conducting strip under a uniform electric current flow and a constant magnetic field (Shindo and Takeuchi, 1988). The crack disturbs the current flow and anti-plane shear stresses are caused by the interaction between the magnetic field and the disturbed current.

The present paper presents an investigation of the stress distribution in a conducting flat plate of finite width containing a finite crack when the plate is subjected to an electric current flow and a magnetic field. The current flow and the magnetic field are uniform and perpendicular to the crack surface, and the crack and the plate surfaces are electrically insulated. The study is based on Mindlin's theory for the flexural motion of plates in which the three physical boundary conditions of vanishing bending moment, twisting moment, and transverse shear force can be satisfied individually at the crack edge (Mindlin, 1951; Embley and Sih, 1973). First, application of the Fourier transform reduces the problem of the electric current density field to the solution of a pair of dual integral equations (Shindo and Takeuchi, 1988; Sneddon, 1951). These equations are solved by using an integral transform technique and the result is expressed in terms of a Fredholm integral equation of the second kind. Next, the electromagneto-elastic field is treated. The interaction between the magnetic field and the disturbed electric current gives rise to an electromagnetic twisting moment to the cracked conducting plate. A solution of the crack problem is obtained by the method of dual integral equations and the result is expressed in terms of a system of simultaneous Fredholm integral equations. The singular parts of the current densities, moments and shear forces are determined in closed elementary forms. Numerical solutions are obtained for the twisting moment intensity factor and the shear force intensity factor, and are displayed graphically as the geometrical parameters are varied.

STATEMENT OF THE PROBLEM AND ELECTRIC CURRENT ANALYSIS

We consider an electrically conducting elastic plate of thickness $2h$ and width $2l$ with fixed ends containing a through crack of length $2a$. The coordinate axes x and y are in the middle plane of the plate, the z-axis is perpendicular to this plane, and the center of the crack is taken as the origin O, as shown in Fig. 1. The cracked conducting plate is permeated by a static uniform magnetic field of magnetic induction B_0 normal to the crack surface. A steady electric current flow passes through the plate, and is uniform and perpendicular to the crack surface. The y component of the undisturbed electric current density vector $\mathbf{J}_e$ is

$$J_{ey} = J_e \tag{1}$$

where J_e is a constant with the dimension of current density. The current flow is disturbed by the presence of the crack and the twisting moment is caused by the interaction between the magnetic field and the disturbed current.

The electric potential $\Phi_e(x, y)$ is

$$\Phi_e(x, y) = -\frac{J_e}{\sigma} y + \varphi_e(x, y), \tag{2}$$

where σ is the electric conductivity. The disturbed electric potential function $\varphi_e(x, y)$ is governed by the following Laplace equation:

$$\varphi_{e,xx} + \varphi_{e,yy} = 0. \tag{3}$$

The nontrivial components of the electric current density vector $\mathbf{J}$ are

$$\begin{aligned} J_x &= -\sigma\Phi_{e,x} = -\sigma\varphi_{e,x}, \\ J_y &= -\sigma\Phi_{e,y} = J_e - \sigma\varphi_{e,y}, \end{aligned} \tag{4}$$

where J_x, J_y are the x, y components of $\mathbf{J}$ and a comma denotes partial differentiation with respect to the coordinate.

The problem is solved for the case of electrically insulated crack and plate surfaces. The electric current density at the ends $y = \pm l$ is assumed to be $J_y = J_e$. Because of the assumed symmetry, it is sufficient to consider the problem for $0 \leqslant x < \infty$, $0 \leqslant y \leqslant l$ only. Therefore the electric boundary conditions are given as:

$$\begin{aligned} \varphi_{e,y} &= J_e/\sigma \quad (y = 0, \quad 0 \leqslant x < a), \\ \varphi_e &= 0 \quad (y = 0, \quad a \leqslant x < \infty), \end{aligned} \tag{5}$$

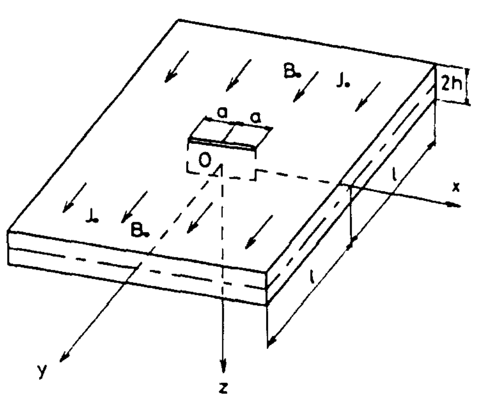

Fig. 1. A conducting plate with a through crack.

$$\varphi_{e,y} = 0 \qquad (y = l, \quad 0 \leqslant x < \infty). \tag{6}$$

A Fourier transform is applied to eqn (3) and the result is

$$\varphi_e = \frac{2}{\pi}\int_0^\infty \{A_1(s)\exp(-sy) + A_2(s)\exp(sy)\}\cos(sx)\,ds, \tag{7}$$

where $A_1(s)$ and $A_2(s)$ are the unknown functions to be determined later. The boundary conditions (6) lead to the following relation between unknown functions:

$$A_2(s) = \exp(-2sl)A_1(s). \tag{8}$$

Making use of the mixed boundary conditions (5), we have a pair of dual integral equations:

$$\int_0^\infty sA_1(s)\sinh(sl)\exp(-sl)\cos(sx)\,ds = -\frac{\pi J_c}{4\sigma} \quad (0 \leqslant x < a),$$

$$\int_0^\infty A_1(s)\cosh(sl)\exp(-sl)\cos(sx)\,ds = 0 \quad (a \leqslant x < \infty). \tag{9}$$

The solution of the dual integral equations (9) may be obtained by using a new function $h(\zeta)$ (Shindo and Takeuchi, 1988) and the result is

$$A_1(s) = -\frac{\pi J_c a^2 \exp(sl)}{4\sigma\cosh(sl)}\int_0^1 \zeta^{1/2}h(\zeta)J_0(sa\zeta)\,d\zeta, \tag{10}$$

where $J_0(\ )$ is the zero-order Bessel function of the first kind and $h(\zeta)$ is the solution to the following Fredholm integral equation of the second kind:

$$h(\zeta) + \int_0^1 h(\eta)K_h(\zeta,\eta)\,d\eta = \zeta^{1/2}, \tag{11}$$

whose kernel being symmetric in ζ and η is

$$K_h(\zeta,\eta) = (\zeta\eta)^{1/2}\int_0^\infty t\{\tanh(tl/a) - 1\}J_0(t\zeta)J_0(t\eta)\,dt. \tag{12}$$

The singular parts of the current densities in the neighborhood of the crack tip are obtained as

$$J_x \sim \frac{J_c a^{1/2}}{(2r_1)^{1/2}}h(1)\sin(\theta_1/2),$$

$$J_y \sim \frac{J_c a^{1/2}}{(2r_1)^{1/2}}h(1)\cos(\theta_1/2), \tag{13}$$

where r_1 and θ_1 are the polar coordinates defined as:

$$r_1 = \{(x-a)^2 + y^2\}^{1/2},$$

$$\theta_1 = \tan^{-1}\left(\frac{y}{x-a}\right). \tag{14}$$

ELECTROMAGNETO-ELASTIC ANALYSIS

The electric current density J_x and the magnetic induction B_0 in the y direction induce the electromagnetic body force $B_0 J_x$ in the z direction and the twisting moment operates the cracked plate. The electromagnetic twisting of a conducting plate with a through crack using the Mindlin's theory (Mindlin, 1951) is considered. In this theory, the rectangular components of the displacement vector are given by

$$u_\alpha = x_3 \phi_\alpha(x_1, x_2),$$
$$u_3 = \phi_3(x_1, x_2), \tag{15}$$

where $x_1 = x$, $x_2 = y$, $x_3 = z$ are the rectangular Cartesian coordinates. Throughout this section, repeated indices imply the summation convention of Einstein. Greek indices take values in the range (1, 2), and ϕ_3 is the normal displacement of the plate and ϕ_α are the rotations of the normals about x_α-axes. The bending and twisting moments can be expressed in terms of ϕ_α as

$$M_{\alpha\beta} = D\frac{1-\nu}{2}\left(\phi_{\alpha,\beta} + \phi_{\beta,\alpha} + \frac{2\nu}{1-\nu}\phi_{\gamma,\gamma}\delta_{\alpha\beta}\right), \tag{16}$$

where $D = 4\mu h^3/\{3(1-\nu)\}$ is the flexural rigidity of the plate, μ is the shear modulus of elasticity and ν is the Poisson's ratio. The shear forces Q_x and Q_y per unit length of the plate are given by

$$Q_\alpha = \kappa^2 \mu h(\phi_{3,\alpha} + \phi_\alpha), \tag{17}$$

where the shear coefficient κ^2 assumes the value $\pi^2/12$.

Making use of eqns (16) and (17), the three equations of motion become

$$\frac{S}{2}[(1-\nu)\phi_{\alpha,\beta\beta} + (1+\nu)\phi_{\beta,\beta\alpha}] - (\phi_\alpha + \phi_{3,\alpha}) = 0,$$
$$\pi^2\mu[\phi_{3,\beta\beta} + \phi_{\beta,\beta}] + 12 B_0 J_x = 0. \tag{18}$$

The transverse shear effect is associated with $S = 6D/\pi^2\mu h$. For a traction-free crack, the quantities $M_{2\alpha}$ and Q_2 must each vanish for $|x| < a$ and $y = 0$. Hence the mixed boundary conditions may be expressed as follows;

$$M_{2\alpha} = 0, \quad Q_2 = 0 \quad (y = 0, \quad 0 \leqslant x < a), \tag{19}$$

$$M_{22} = 0, \quad \phi_1 = 0, \quad \phi_3 = 0 \quad (y = 0, \quad a \leqslant x < \infty), \tag{20}$$

$$\phi_\alpha = 0, \quad \phi_3 = 0 \quad (y = l, \quad 0 \leqslant x < \infty). \tag{21}$$

A Fourier transform is applied to eqns (18) and the solutions in a rectangular Cartesian coordinate system (x, y, z) are

$$\phi_x = \frac{2}{\pi}\int_0^\infty [s[-\{C_1(s) + C_2(s)(2Ss + y)\}\exp(sy)$$
$$+\{-C_3(s) + C_4(s)(2Ss - y)\}\exp(-sy)]$$
$$+4\lambda(s)(h/\pi)^2[B_1(s)\exp\{\lambda(s)y\} - B_2(s)\exp\{-\lambda(s)y\}]]\cos(sx)\,ds$$
$$+\frac{2}{\pi}\left(\frac{\sigma h B_0}{4D}\right)\int_0^c [(-2S - 8S^2s^2 + 4Ssy - y^2)\exp(-sy)$$

$$-(2S+8S^2s^2+4Ssy+y^2)\exp\{-s(2l-y)\}$$
$$+sH_b(s)(2Ss-y)\exp(-sy)$$
$$-sH_c(s)(2Ss+y)\exp(sy)$$
$$+2sH_d(s)\sinh(sy)$$
$$+2\lambda(s)H_a(s)\sinh\{\lambda(s)y\}]A_1(s)\cos(sx)\,ds,$$

$$\phi_y=\frac{2}{\pi}\int_0^{\infty}[\{-sC_1(s)-C_2(s)(1+2Ss^2+sy)\}\exp(sy)$$
$$+\{sC_3(s)-C_4(s)(1+2Ss^2-sy)\}\exp(-sy)$$
$$+4s(h/\pi)^2[B_1(s)\exp\{\lambda(s)y\}+B_2(s)\exp\{-\lambda(s)y\}]]\sin(sx)\,ds$$
$$+\frac{2}{\pi}\left(\frac{\sigma hB_0}{4D}\right)\int_0^{\infty}[\{6Ss+8S^2s^3-2(1+2Ss^2)y+sy^2\}\frac{1}{s}\exp(-sy)$$
$$-\{6Ss+8S^2s^3+2(1+2Ss^2)y+sy^2\}\frac{1}{s}\exp\{-s(2l-y)\}$$
$$-H_b(s)(1+2Ss^2-sy)\exp(-sy)$$
$$-H_c(s)(1+2Ss^2+sy)\exp(sy)$$
$$+2sH_d(s)\cosh(sy)$$
$$+2sH_a(s)\cosh\{\lambda(s)y\}]A_1(s)\sin(sx)\,ds,$$

$$\phi_z=\frac{2}{\pi}\int_0^{\infty}[\{C_1(s)+C_2(s)y\}\exp(sy)$$
$$+\{C_3(s)+C_4(s)y\}\exp(-sy)]\sin(sx)\,ds$$
$$+\frac{2}{\pi}\left(\frac{\sigma hB_0}{4D}\right)\int_0^{\infty}\left[\frac{y^2}{s}[\exp(-sy)+\exp\{-s(2l-y)\}]\right.$$
$$+y\{H_b(s)\exp(-sy)+H_c(s)\exp(sy)\}$$
$$\left.-2H_d(s)\sinh(sy)\right]A_1(s)\sin(sx)\,ds, \tag{22}$$

where $B_1(s)$, $B_2(s)$ and $C_1(s)$, $C_2(s)$, $C_3(s)$, $C_4(s)$ are the unknowns to be solved, and $\lambda(s)$ and $H_a(s)$, $H_b(s)$, $H_c(s)$, $H_d(s)$ are given in Appendix A.

Making use of the boundary conditions (19)–(21) renders

$$s\{C_1(s)+C_3(s)\}+2\left(\frac{1}{1-\nu}+Ss^2\right)\{C_2(s)-C_4(s)\}$$
$$-\lambda(s)(2h/\pi)^2\{B_1(s)-B_2(s)\}=0,$$
$$-s\{\exp(sl)C_1(s)+\exp(-sl)C_3(s)\}$$
$$-(sl+2Ss^2)\exp(sl)C_2(s)+(-sl+2Ss^2)\exp(-sl)C_4(s)$$
$$+\lambda(s)(2h/\pi)^2[\exp\{\lambda(s)l\}B_1(s)-\exp\{-\lambda(s)l\}B_2(s)]=0,$$
$$-s\{\exp(sl)C_1(s)-\exp(-sl)C_3(s)\}$$
$$-(1+sl+2Ss^2)\exp(sl)C_2(s)-(1-sl+2Ss^2)\exp(-sl)C_4(s)$$
$$+s(2h/\pi)^2[B_1(s)\exp\{\lambda(s)l\}+B_2(s)\exp\{-\lambda(s)l\}]=0,$$
$$\exp(sl)C_1(s)+\exp(-sl)C_3(s)+l\{\exp(sl)C_2(s)+\exp(-sl)C_4(s)\}=0, \tag{23}$$

$$\int_0^\infty \left[\{s+f_{11}(s)\} D_1(s) + \frac{2}{1-\nu} f_{12}(s) D_2(s) \right] \sin(sx)\,ds$$

$$= 4S\left(\frac{\sigma h B_0}{4D}\right) \int_0^\infty F_1(s) A_1(s) \sin(sx)\,ds \quad (0 \leqslant x < a),$$

$$\int_0^\infty D_1(s) \sin(sx)\,ds = 0 \quad (a \leqslant x < \infty). \tag{24}$$

$$\int_0^\infty \left[f_{21}(s) D_1(s) + \frac{2}{1-\nu} \{(1+\nu)s + f_{22}(s)\} D_2(s) \right] \cos(sx)\,ds$$

$$= \left(\frac{\sigma h B_0}{4D}\right) \int_0^\infty F_2(s) A_1(s) \cos(sx)\,ds \quad (0 \leqslant x < a),$$

$$\int_0^\infty D_2(s) \cos(sx)\,ds = 0 \quad (a \leqslant x < \infty). \tag{25}$$

Equations (24) and (25) are the simultaneous dual integral equations and the functions $f_{ij}(s)$ $(i, j = 1, 2)$ and $F_l(s)$ $(l = 1, 2)$ are given in Appendix B. The unknowns $D_1(s)$ and $D_2(s)$ are related $C_i(s)$ $(i = 1$–$4)$ as follows:

$$D_1(s) = C_1(s) + C_3(s),$$
$$D_2(s) = C_2(s) - C_4(s). \tag{26}$$

In order to solve the simultaneous dual integral equations (24), (25), we introduce the representations:

$$D_1(s) = \frac{\pi}{2} S\left(\frac{h B_0 J_c}{4D}\right) a^3 \int_0^1 \xi^{1/2} \psi_1(\xi) J_1(sa\xi)\,d\xi,$$

$$D_2(s) = \frac{\pi}{2}\left(\frac{h B_0 J_c}{4D}\right) a^4 \int_0^1 \xi^{1/2} \psi_2(\xi) J_0(sa\xi)\,d\xi, \tag{27}$$

where $J_1(\ )$ is the first-order Bessel function of the first kind. The second equations of (24) and (25) are satisfied identically by the integral representations (27). If we now substitute eqns (27) into the first equations of (24) and (25), after some manipulations, we have the following simultaneous Fredholm integral equations of the second kind:

$$\psi_1(\xi) + \int_0^1 \psi_1(\eta) K_{11}(\xi,\eta)\,d\eta + \int_0^1 \psi_2(\eta) K_{12}(\xi,\eta)\,d\eta = \int_0^1 h(\zeta) K_{13}(\xi,\zeta)\,d\zeta,$$

$$\int_0^1 \psi_1(\eta) K_{21}(\xi,\eta)\,d\eta + \psi_2(\xi) + \int_0^1 \psi_2(\eta) K_{22}(\xi,\eta)\,d\eta = \int_0^1 h(\zeta) K_{23}(\xi,\zeta)\,d\zeta. \tag{28}$$

The kernels $K_{ij}(\xi, \eta)$ $(i = 1, 2;\ j = 1$–$3)$ take the forms:

$$K_{11}(\xi,\eta) = (\xi\eta)^{1/2}\int_0^\infty f_{1a}(t)J_1(t\xi)J_1(t\eta)\,dt,$$

$$K_{12}(\xi,\eta) = (\xi\eta)^{1/2}\left(\frac{\pi a}{2h}\right)^2\int_0^\infty f_{1b}(t)J_1(t\xi)J_0(t\eta)\,dt,$$

$$K_{21}(\xi,\eta) = \frac{1}{1+\nu}(\xi\eta)^{1/2}\left(\frac{2h}{\pi a}\right)^4\int_0^\infty f_{2a}(t)J_0(t\xi)J_1(t\eta)\,dt,$$

$$K_{22}(\xi,\eta) = \frac{1}{1+\nu}(\xi\eta)^{1/2}\int_0^\infty f_{2b}(t)J_0(t\xi)J_0(t\eta)\,dt, \tag{29}$$

$$K_{13}(\xi,\zeta) = -4(\xi\zeta)^{1/2}\int_0^\infty \frac{F_a(t)}{1+\exp(-2tl/a)}J_1(t\xi)J_0(t\zeta)\,dt,$$

$$K_{23}(\xi,\zeta) = -\frac{1-\nu}{2(1+\nu)}(\xi\zeta)^{1/2}\int_0^\infty \frac{F_b(t)}{1+\exp(-2tl/a)}J_0(t\xi)J_0(t\zeta)\,dt, \tag{30}$$

where $f_{1a}(t)$, $f_{1b}(t)$, $f_{2a}(t)$, $f_{2b}(t)$ and $F_a(t)$, $F_b(t)$ are given in Appendix C.

The singular parts of the moments and shear forces in the neighborhood of the crack tip can be determined from the asymptotic solution expressed in terms of a set of polar coordinates r_1 and θ_1. The final results are

$$\begin{bmatrix} M_{xx} \\ M_{yy} \\ M_{xy} \end{bmatrix} \sim \frac{k_2}{(2r_1)^{1/2}}\begin{bmatrix} -\frac{7}{8}\sin(\theta_1/2)-\frac{1}{8}\sin(5\theta_1/2) \\ -\frac{1}{8}\sin(\theta_1/2)+\frac{1}{8}\sin(5\theta_1/2) \\ \frac{3}{4}\cos(\theta_1/2)+\frac{1}{4}\cos(5\theta_1/2) \end{bmatrix}, \tag{31}$$

$$\begin{bmatrix} Q_x \\ Q_y \end{bmatrix} \sim \frac{k_3}{(2r_1)^{1/2}}\begin{bmatrix} -\sin(\theta_1/2) \\ \cos(\theta_1/2) \end{bmatrix}. \tag{32}$$

The twisting moment intensity factor k_2 and the shear force intensity factor k_3 may be defined as

$$\begin{aligned} k_2 &= \lim_{x\to a^+}[\{2(x-a)\}^{1/2}M_{yx}(x,0)] \\ &= 2(1+\nu)(hB_0J_c)a^{5/2}\psi_2(1), \end{aligned} \tag{33}$$

$$\begin{aligned} k_3 &= \lim_{x\to a^+}[\{2(x-a)\}^{1/2}Q_y(x,0)] \\ &= -2(hB_0J_c)a^{3/2}\psi_1(1). \end{aligned} \tag{34}$$

NUMERICAL RESULTS AND DISCUSSION

In order to evaluate the twisting moment intensity factor k_2 and the shear force intensity factor k_3 it is necessary first to numerically solve the Fredholm integral equation (11) for $h(\eta)$ and the simultaneous Fredholm integral equations (28) for $\psi_1(\eta)$, $\psi_2(\eta)$. Figure 2 exhibits the variation of the normalized twisting moment intensity factor $k_2/B_0J_0a^{7/2}$ against the l/a ratio. The Poisson's ratio ν is taken to be $\nu = 0.3$. $k_2/B_0J_0a^{7/2}$ increases more rapidly with the l/a ratio when the h/a ratio is increased. The effect of the Poisson's ratio ν on the twisting moment intensity factor is shown in Fig. 3 for $h/a = 0.5$. A smaller value of ν tends to increase $k_2/B_0J_0a^{7/2}$ for a given l/a.

Figure 4 shows a plot of the normalized shear force intensity factor $k_3/B_0J_0a^{5/2}$ in eqn (34) versus the l/a ratio for $\nu = 0.3$ and $h/a = 0.25$, 0.50, 0.75. It is seen that the k_3 values increase at first reaching a maximum with the l/a ratio, and approach the values for $l/a = \infty$.

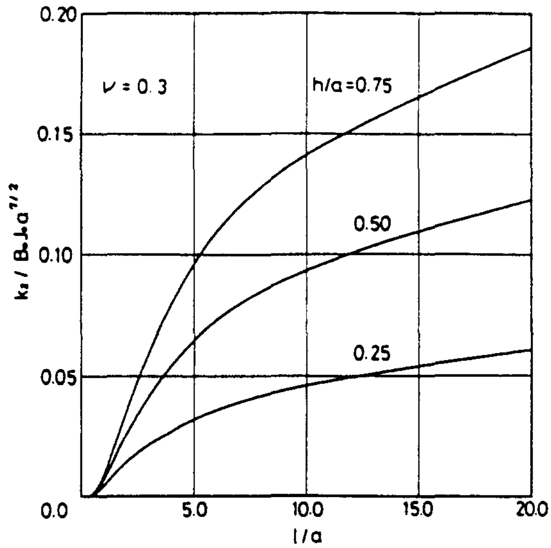

Fig. 2. Twisting moment intensity factor $k_2/B_0J_0a^{7/2}$ versus l/a for $h/a = 0.25$, 0.50 and 0.75.

Decreasing plate thickness h/a tends to lower the k_3 value. As the ratio $h/a \to \infty$ and the ratio $l/a \to \infty$, k_3 tends to the solution

$$k_3 = \frac{hB_0J_0}{2}a^{3/2}. \tag{35}$$

The stress intensity factor of an infinite medium with a finite crack under electromagnetic antiplane shear load is given by $(B_0J_0/4)a^{3/2}$ (Shindo and Takeuchi, 1988). The shear force Q_y per unit length of the plate is defined, in terms of the stress component, as

$$Q_y = \int_{-h}^{h} \sigma_{yz}\,dz. \tag{36}$$

Making use of eqn (36), the stress intensity factor $(B_0J_0/4)a^{3/2}$ may be converted to the following shear force intensity factor:

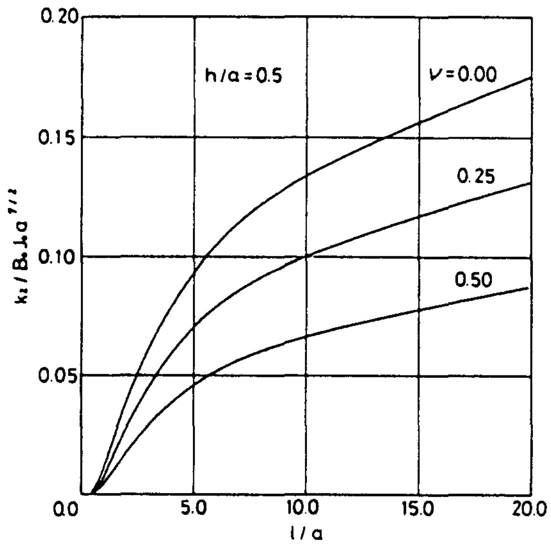

Fig. 3. Effect of Poisson's ratio ν on twisting moment intensity factor $k_2/B_0J_0a^{7/2}$ for $h/a = 0.5$.

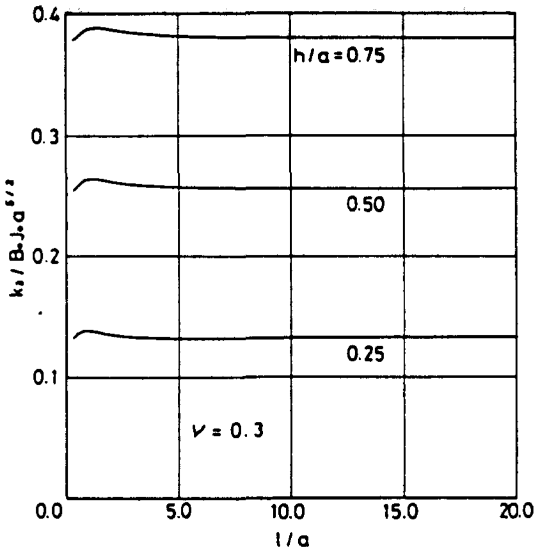

Fig. 4. Shear force intensity factor $k_3/B_0J_0a^{3/2}$ versus l/a for $h/a = 0.25$, 0.50 and 0.75.

$$k_3 = \int_{-h}^{h} \frac{B_0J_0}{4} a^{3/2}\,dz = \frac{hB_0J_0}{2} a^{3/2}, \tag{37}$$

which agrees with eqn (35).

In conclusion, the electromagneto-elastic analysis of a conducting plate of finite width with a through crack under a current flow and a magnetic field has been shown in this study. The results are expressed in terms of the twisting moment intensity factor and the shear force intensity factor. It is found that the twisting moment intensity factor increases with the plate-width to the crack length ratio l/a, depending on the perturbation of the electric current field, the plate-thickness to the crack length ratio h/a and the Poisson's ratio ν. The shear force intensity factor is also given as a function of the ratio l/a for different ratios of h/a and $\nu = 0.3$, and the results depend on the perturbation of the electric current field. The larger values of the parameters h/a and l/a will give the worst scenario for design purposes.

Acknowledgement—This work was supported in part by the Scientific Research Fund of the Ministry of Education for the fiscal year 1990.

REFERENCES

Embley, G. T. and Sih, G. C. (1973). Sudden appearance of a crack in a bent plate. *Int. J. Solids Structures* **9**, 1349–1359.
Mindlin, R. D. (1951). Influence of rotary inertia and shear on flexural motions of isotropic elastic plates. *ASME J. Appl. Mech.* **18**, 31–38.
Murakami, Y. (1986). *Stress Intensity Factors Handbook*, Vols 1, 2. Pergamon Press, Oxford.
Shindo, Y. and Takeuchi, A. (1988). Singular stresses of a finite crack in an elastic conducting strip under electromagnetic force. *Fusion Engng Design* **6**, 199–205.
Sneddon, I. N. (1951). *Fourier Transforms*. McGraw-Hill, New York.

APPENDIX A

$$\lambda(s) = \{s^2 + (\pi/2h)^2\}^{1/2}, \tag{A1}$$

$$H_a(s) = -l\left\{\frac{1}{\tanh(sl)} - \frac{1}{s}\right\}\frac{1}{H_{a0}(s)},$$

$$H_b(s) = \left[\lambda(s)H_a(s)\frac{\sinh\{\lambda(s)l\}}{\sinh(sl)} + 2(Y_t + 4Y_t^2s^2)\right]\frac{1}{2Y_ts^2},$$

$$H_c(s) = H_b(s) - \left(\frac{1}{s^2} + 4Y_t\right)\{1 + \exp(-2-sl)\},$$

$$H_d(s) = l\left[\left\{H_b(s) - \left(\frac{1}{s^2} + 4Y_t\right)\right\}\{1 + \exp(-2sl)\} + \frac{2l}{s}\exp(-2sl)\right]\frac{1}{1 - \exp(-2sl)}, \tag{A2}$$

$$H_{a0}(s) = \exp\{\lambda(s)l\} + \frac{2\lambda(s)}{Y_c s^2}[\exp\{\lambda(s)l\} - \exp(sl)]\left\{\frac{sl}{\sinh(sl)} - (2Y_c s^2 + 1)\cosh(sl)\right\}\frac{1}{\sinh(sl)}. \quad \text{(A3)}$$

The quantity Y_c stands for

$$Y_c = \frac{6D}{\pi^2 \mu h}. \quad \text{(A4)}$$

APPENDIX B

$$f_{11}(s) = -\left(\frac{\pi}{2h}\right)^2 \frac{s}{\lambda(s)\{\lambda(s)+s\}} + \left\{\frac{2s^2}{\lambda(s)}\right\}\frac{\exp\{-2\lambda(s)l\}}{1-\exp\{-2\lambda(s)l\}}$$
$$+ \frac{4Ss^2}{l}\left[\frac{G_1(s)}{G_3(s)}\{1-\exp(-2sl)\} - 1\right]\left[\frac{1}{1+\exp(-2sl)} - \frac{s\tanh(sl)\exp[\{s-\lambda(s)\}l]}{1-\exp\{-2\lambda(s)l\}}\right],$$

$$f_{12}(s) = \left(\frac{\pi}{2h}\right)^2 \frac{s}{\lambda(s)\{\lambda(s)+s\}^2} + (1-\nu)\left[2Ss^2\frac{\exp(-2sl)}{1+\exp(-2sl)}\right.$$
$$\left.+ \frac{s}{\lambda(s)}\left(2Ss^2 + \frac{2}{1-\nu}\right)\frac{\exp\{-2\lambda(s)l\}}{1-\exp\{-2\lambda(s)l\}}\right] + 2(1-\nu)Ss^2$$
$$\times\left[\frac{s\exp[\{s-\lambda(s)\}l]}{\lambda(s)[1-\exp\{-2\lambda(s)l\}]}\{\tanh(sl)-1\} + \frac{G_2(s)}{G_3(s)}\left\{\frac{\tanh(sl)}{l}\right\}\right.$$
$$\left.\times\left[1 - \frac{s\exp[\{s-\lambda(s)\}l]}{\lambda(s)\{1-\exp\{-2\lambda(s)l\}\}}\{1-\exp(-2sl)\}\right]\right],$$

$$f_{21}(s) = \left(\frac{\pi}{2h}\right)^2 \frac{s}{\lambda(s)\{\lambda(s)+s\}^2} - 4s^2\left\{\frac{G_1(s)}{G_3(s)} - 1\right\}$$
$$+ 2[\{\lambda(s)\}^2 + s^2]\left\{\frac{s}{\lambda(s)}\right\}\frac{\exp\{-2\lambda(s)l\}}{1-\exp\{-2\lambda(s)l\}} + \frac{4s}{l\{1+\exp(-2sl)\}}$$
$$\times\left[\frac{G_1(s)}{G_3(s)}\{1-\exp(-2sl)\} - 1\right]\left[2Ss^2 + 1 - \frac{\{\lambda(s)\}^2+s^2}{\lambda(s)}\exp[\{s-\lambda(s)\}l]Ss\tanh(sl)\right],$$

$$f_{22}(s) = \left(\frac{\pi}{2h}\right)^2 \frac{\{\lambda(s)\}^2+s^2}{\lambda(s)\{\lambda(s)+s\}^2} + 2(1-\nu)s(2Ss^2+1)\frac{\exp(-2sl)}{1+\exp(-2sl)}$$
$$+ (1-\nu)\frac{\{\lambda(s)\}^2+s^2}{\lambda(s)}\left[\left(2Ss^2 + \frac{2}{1-\nu}\right)\frac{\exp\{-2\lambda(s)l\}}{1-\exp\{-2\lambda(s)l\}}\right.$$
$$\left.+ 2Ss^2\frac{\exp[\{s-\lambda(s)\}l]}{1-\exp\{-2\lambda(s)l\}}\{\tanh(sl)-1\}\right] + (1-\nu)\frac{G_2(s)}{G_3(s)}\left[2s\{(2Ss^2+1)\tanh(sl) - sl\}\right.$$
$$\left.- 2Ss^2[\{\lambda(s)\}^2+s^2]\frac{\exp[\{s-\lambda(s)\}l]}{\lambda(s)[1-\exp\{-2\lambda(s)l\}]}\{1-\exp(-2sl)\}\tanh(sl)\right], \quad \text{(B1)}$$

$$G_1(s) = sl\{1-\tanh(sl)\} - 2Ss^2 - 1 + 2Ss^3\frac{\tanh(sl)}{\lambda(s)\tanh\{\lambda(s)l\}} - \frac{s^2 l}{\lambda(s)}\left[1 - \frac{1}{\tanh\{\lambda(s)l\}}\right]\exp[\{\lambda(s)-s\}l],$$

$$G_2(s) = \{1-\tanh(sl)\}\left[sl - 2Ss^3\frac{1}{\lambda(s)\tanh\{\lambda(s)l\}}\right] - \left(2Ss^2 + \frac{2}{1-\nu}\right)\left[1 - \frac{1}{\tanh\{\lambda(s)l\}}\right]\frac{s}{\lambda(s)}\exp[\{\lambda(s)-s\}l],$$

$$G_3(s) = sl[\{1+\exp(-2sl)\} - \tanh(sl)\{1-\exp(-2sl)\}]$$
$$-\{1-\exp(-2sl)\}\left[2Ss^2 + 1 - 2Ss^3\frac{\tanh(sl)}{\lambda(s)\tanh\{\lambda(s)l\}}\right]. \quad \text{(B2)}$$

$$F_1(s) = 4S\left\{1 - \exp(-2sl) + \frac{E_3(s)}{E_1(s)}\right\},$$

$$F_2(s) = 8l\left\{\frac{E_2(s)}{E_1(s)} + \frac{sl}{1-\exp(-2sl)}\right\}\exp(-2sl) - \frac{2}{s}\{1-\exp(-2sl)\}. \quad \text{(B3)}$$

$$E_1(s) = \lambda(s)[1-\exp\{-2\lambda(s)l\}]E_{1a}(s)+2Ss^3[1+\exp\{-2\lambda(s)l\}]\{1-\exp(-2sl)\},$$

$$E_2(s) = \lambda(s)[1-\exp\{-2\lambda(s)l\}]\left\{\frac{sl}{\tanh(sl)}-1\right\}\left\{\frac{sl}{\tanh(sl)}-1-2Ss^2\right\},$$

$$E_3(s) = 2sl\left\{\frac{sl}{\tanh(sl)}-1\right\}[s\{1-\exp(-2sl)\}$$
$$-\lambda(s)\exp[\{\lambda(s)-s\}l][1-\exp\{-2\lambda(s)l\}]]\exp[-\{s+\lambda(s)\}l]. \quad (B4)$$

$$E_{1a}(s) = sl\left\{\frac{1+\exp(-2sl)}{\tanh(sl)}-1+\exp(-2sl)\right\}-(2Ss^2+1)\{1+\exp(-2sl)\}. \quad (B5)$$

APPENDIX C

$$f_{1a}(t) = -\left(\frac{\pi a}{2h}\right)^2\frac{t}{\lambda_0(t)\{\lambda_0(t)+t\}}+\left\{\frac{2t^2}{\lambda_0(t)}\right\}\frac{\exp\{-2\lambda_0(t)(l/a)\}}{1-\exp\{-2\lambda_0(t)(l/a)\}}+\frac{4S_0t^2}{(l/a)}\left[\frac{G_a(t)}{G_c(t)}\{1-\exp(-2tl/a)\}-1\right]$$
$$\times\left[\frac{1}{1+\exp(-2tl/a)}-\frac{t\tanh(tl/a)\exp[\{t-\lambda_0(t)\}l/a]}{\lambda_0(t)[1-\exp\{2\lambda_0(t)l/a\}]}\right],$$

$$f_{1b}(t) = \left(\frac{\pi a}{2h}\right)^2\frac{t}{\lambda_0(t)\{\lambda_0(t)+t\}^2}+(1-\nu)\left[2S_0t^2\frac{\exp(-2tl/a)}{1+\exp(-2tl/a)}\right.$$
$$\left.+\frac{t}{\lambda_0(t)}\left(2S_0t^2+\frac{2}{1-\nu}\right)\frac{\exp\{-2\lambda_0(t)l/a\}}{1-\exp\{-2\lambda_0(t)l/a\}}\right]$$
$$+2(1-\nu)S_0t^2\left[\frac{t\exp[\{t-\lambda_0(t)\}l/a]}{\lambda_0(t)[1-\exp\{-2\lambda_0(t)l/a\}]}\{\tanh(tl/a)-1\}+\frac{G_b(t)}{G_c(t)}\left\{\frac{\tanh(tl/a)}{(l/a)}\right\}\right.$$
$$\left.\times\left[1-\frac{t\exp[\{t-\lambda_0(t)\}l/a]}{\lambda_0(t)[1-\exp\{2\lambda_0(t)l/a\}]}\{1-\exp(-2tl/a)\}\right]\right],$$

$$f_{2a}(t) = \left(\frac{\pi a}{2h}\right)^4\frac{t}{\lambda_0(t)\{\lambda_0(t)+t\}^2}-4t^2\left\{\frac{G_a(t)}{G_c(t)}-1\right\}$$
$$+2[\{\lambda_0(t)\}^2+t^2]\left\{\frac{t}{\lambda_0(t)}\right\}\frac{\exp\{-2\lambda_0(t)l/a\}}{1-\exp\{-2\lambda_0(t)l/a\}}$$
$$+\frac{4t}{(l/a)\{1+\exp(-2tl/a)\}}\left[\frac{G_a(t)}{G_c(t)}\{1-\exp(-2tl/a)\}-1\right]$$
$$\times\left[2S_0t^2+1-\frac{\{\lambda_0(t)\}^2+t^2}{\lambda_0(t)}\exp[\{t-\lambda_0(t)\}l/a]S_0t\tanh(tl/a)\right],$$

$$f_{2b}(t) = \left(\frac{\pi a}{2h}\right)^2\frac{\{\lambda_0(t)\}^2+t^2}{\lambda_0(t)\{\lambda_0(t)+t\}^2}+2(1-\nu)t(2S_0t^2+1)\frac{\exp(-2tl/a)}{1+\exp(-2tl/a)}$$
$$+(1-\nu)\frac{\{\lambda_0(t)\}^2+t^2}{\lambda_0(t)}\left[\left(2S_0t^2+\frac{2}{1-\nu}\right)\frac{\exp\{-2\lambda_0(t)l/a\}}{1-\exp\{-2\lambda_0(t)l/a\}}\right.$$
$$\left.+2S_0t^2\frac{\exp[\{t-\lambda_0(t)\}l/a]}{1-\exp\{-2\lambda_0(t)l/a\}}\{\tanh(tl/a)-1\}\right]$$
$$+(1-\nu)\frac{G_b(t)}{G_c(t)}\left[2t\{(2S_0t^2+1)\tanh(tl/a)-tl/a\}-2S_0t^2[\{\lambda_0(t)\}^2+t^2]\right.$$
$$\left.\times\frac{\exp[\{t-\lambda_0(t)\}l/a]}{\lambda_0(t)[1-\exp\{-2\lambda_0(t)l/a\}]}\{1-\exp(-2tl/a)\}\tanh(tl/a)\right]. \quad (C1)$$

$$G_a(t) = (tl/a)\{1-\tanh(tl/a)\}-2S_0t^2-1+2S_0t^3\frac{\tanh(tl/a)}{\lambda_0(t)\tanh\{\lambda_0(t)l/a\}}$$
$$-\frac{t^2(l/a)}{\lambda_0(t)}\left[1-\frac{1}{\tanh\{\lambda_0(t)l/a\}}\right]\exp[\{\lambda_0(t)-t\}l/a],$$

$$G_h(t) = \{1-\tanh(tl/a)\}\left[tl/a - 2S_0t^3\frac{1}{\lambda_0(t)\tanh\{\lambda_0(t)l/a\}}\right] - \left(2S_0t^2+\frac{2}{1-\nu}\right)\left[1-\frac{1}{\tanh\{\lambda_0(t)l/a\}}\right]\frac{t}{\lambda_0(t)}\exp\left[\{\lambda_0(t)-t\}l/a\right].$$

$$G_c(t) = (tl/a)[1+\exp(-2tl/a)-\tanh(tl/a)\{1-\exp(-2tl/a)\}] - \{1-\exp(-2tl/a)\}\left[2S_0t^2+1-2S_0t^3\frac{\tanh(tl/a)}{\lambda_0(t)\tanh\{\lambda_0(t)l/a\}}\right]. \quad (C2)$$

$$\lambda_0(t) = \left\{t^2+\left(\frac{\pi a}{2h}\right)^2\right\}^{1/2}. \quad (C3)$$

$$S_0 = \frac{8}{1-\nu}\left(\frac{h}{\pi a}\right)^2. \quad (C4)$$

$$F_a(t) = 4S_0\left[\{1-\exp(-2tl/a)\}+\frac{E_{30}(t)}{E_{10}(t)}\right].$$

$$F_b(t) = 8(l/a)\left\{\frac{E_{30}(t)}{E_{20}(t)}+\frac{t(l/a)}{1-\exp(-2tl/a)}\right\}\exp(-2tl/a) - \frac{2}{t}\{1-\exp(-2tl/a)\}. \quad (C5)$$

$$E_{10}(t) = \lambda_0(t)[1-\exp\{-2\lambda_0(t)l/a\}]E_{1h}(t)+2S_0t^3[1+\exp\{-2\lambda_0(t)l/a\}]\{1-\exp(-2tl/a)\},$$

$$E_{20}(t) = \lambda_0(t)[1-\exp\{-2\lambda_0(t)l/a\}]\left\{\frac{t(l/a)}{\tanh(tl/a)}-1-2S_0t^2\right\},$$

$$E_{30}(t) = 2t(l/a)\left\{\frac{t(l/a)}{\tanh(tl/a)}-1\right\}[t\{1-\exp(-2tl/a)\} - \lambda_0(t)\exp[\{\lambda_0(t)-t\}l/a][1-\exp\{-2\lambda_0(t)l/a\}]]\exp[-\{t+\lambda_0(t)\}l/a]. \quad (C6)$$

$$E_{1h}(t) = t(l/a)\left\{\frac{1+\exp(-2tl/a)}{\tanh(tl/a)}-1+\exp(-2tl/a)\right\}-(2S_0t^2+1)\{1+\exp(-2tl/a)\}. \quad (C7)$$